Arab J Geosci (2016) 9: 14
DOI 10.1007/s12517-015-2110-2

ORIGINAL PAPER

Late cretaceous mantle plume activity in Ceno-Tethys: evidences from the Hamrani volcanic rocks, western Pakistan

Rehanul Haq Siddiqui[1] · **M. Qasim Jan**[2] · **M. Ishaq Kakar**[3] · **Ehsanullah Kakar**[1] · **Asif Hanif Chaudhary**[4] · **Sikandar Ali Baig**[4]

Received: 13 April 2015 / Accepted: 10 September 2015 / Published online: 8 December 2015

Abstract Basaltic pillow lavas from near the Muslim Bagh town in northern Balochistan are found in the tectonic slivers of the Bagh Complex, northwest of Muslim Bagh Ophiolite. These volcanic rocks are mainly basanites and tephrites. Their petrography and chemistry suggest that these belong to the mildly–strongly alkaline, intra-plate volcanic rock series. Their low Mg # and low Cr, Ni, and Co contents suggest that the parent magma of these volcanic rocks was not directly derived from a partially melted mantle source but have been modified by fractionation en route to eruption. Their primordial mantle-normalized trace element patterns show enrichment in large ion lithophile elements (LILE) and in high field strength elements (HFSE), with marked positive Nb anomalies, and further confirm their within-plate geochemical signatures consistent with an enriched mantle source. Modeling of their Zr versus Zr/Y trends suggest that these volcanic rocks were derived from about 10–15 % melting of an enriched OIB-style mantle source. It is suggested that these Late Cretaceous intra-plate volcanic rocks may represent the mantle plume activity possibly of the Reunion hotspot. These may have erupted on the Ceno-Tethys Ocean floor prior to the passage of Indian plate over it with subsequent tectonic imbrication during Ceno-Tethyan closure and collision with the Eurasian margin.

Keywords Late Cretaceous · Alkaline volcanic rocks · Ceno-Tethys Ocean · North-western Pakistan

✉ Rehanul Haq Siddiqui
rehanhs1@gmail.com

[1] Balochistan University of Information Technology, Engineering and Management Sciences, Quetta, Pakistan

[2] National Centre of Excellence in Geology, University of Peshawar, & COMSTECH, Islamabad, Pakistan

[3] Centre of Excellence in Mineralogy, University of Balochistan, Quetta, Pakistan

[4] Geoscience Advance Research Laboratories, Geological Survey of Pakistan, Shahzad Town, Islamabad, Pakistan

Introduction

The igneous rocks are generated mostly at divergent and convergent plate margins, but there are exceptional sites of volcanism where they are generated within plates by hotspots; areas in the earth's mantle where columns of hot magma rise up to melt through the crust, resulting in igneous activity (e.g., Wilson 1963). Along with magmatic activity of convergent margin in the Chagai-Ras Koh magmatic arc (e.g., Siddiqui et al. 2015) and the divergent setting in Bela–Muslim Bagh–Waziristan ophiolites belt (Kakar et al. 2014a, b). the geology of western and north-western Pakistan is also characterized by the intra-plate volcanic activity (e.g., Khan et al. 1999). These rocks are found intruded in the Indian continent passive margin sediments: Jurassic Alozai Group (Kerr et al. 2010). Cretaceous Parh Group (Mahoney et al. 2002). and the subduction-accretion complexes found beneath the ophiolites (Gnos et al. 1998; Kakar et al. 2014a).

The Muslim Bagh Ophiolite is one of the largest ophioites in Pakistan and is underlain by an accretionary-wedge complex known as Bagh Complex. This complex comprises Mesozoic sedimentary, igneous, and metamorphic assemblages and is exposed around the Muslim Bagh Ophiolite (Fig. 1). The geology, biostratigraphy, and tectonics of this complex have already been reported by many workers (e.g., Otsuki et al. 1989; Kojima et al. 1994; Kimura et al. 1993; Naka et al. 1996 and Kakar et al. 2014a). The volcanic rocks of the Bagh Complex are identified as mid-oceanic ridge

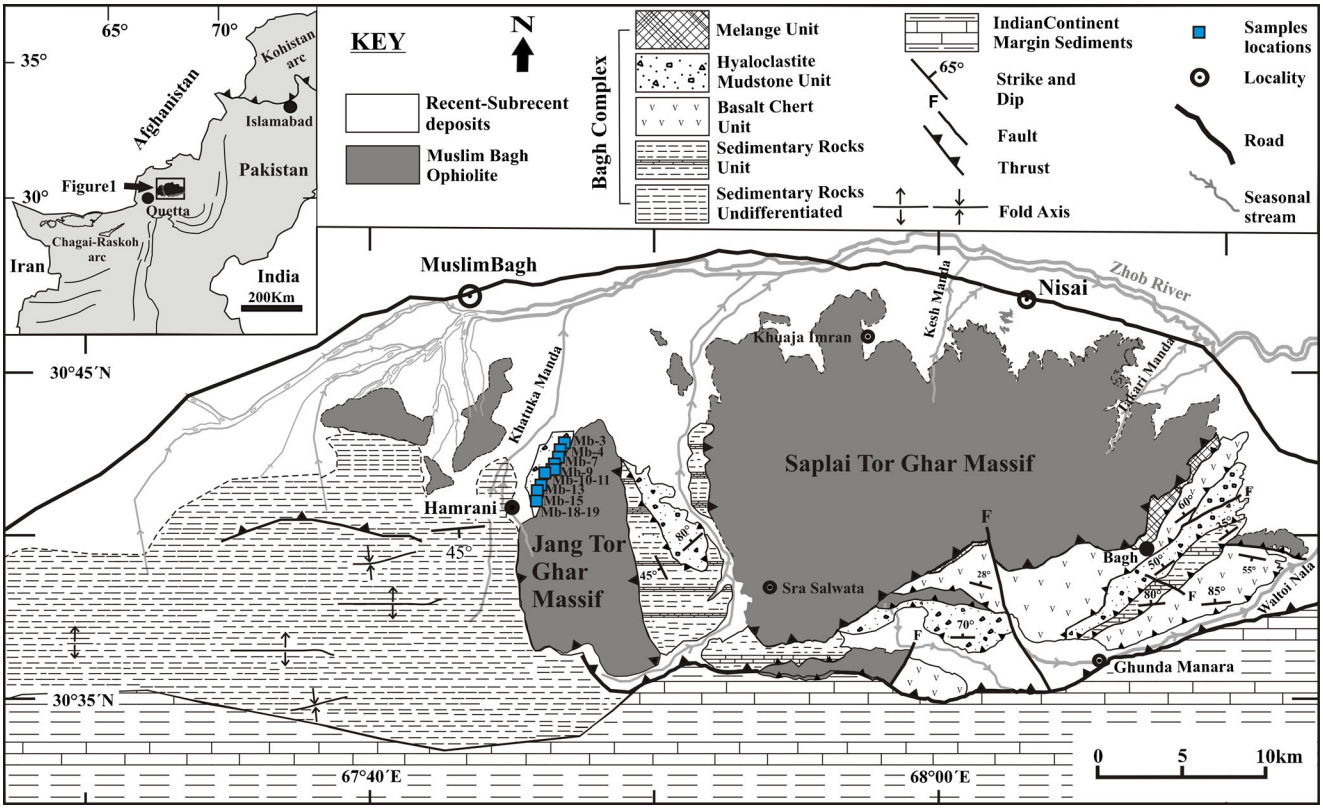

Fig. 1 Geological map of the Muslim Bagh area north-western Pakistan showing the locations of the Hamrani volcanic rocks (modified after Siddiqui et al. 2011; Kakar et al. 2014a)

basalts (MORBs) and oceanic island basalts (OIBs) (Sawada et al. 1992). The petrogenesis of both types of the basalts is well documented in Kakar et al. (2014a). The petrogenetic model of the OIB-type basalts with reference to the regional tectonic reconstruction was still waited. This paper presents a brief account of geological, petrographic, and petrogenetic aspects of Hamrani volcanic rocks and relates their emplacement with mantle plume activity on the Ceno-Tethys Ocean floor prior to the passage of Indian plate over it.

Geology and petrography

The Bagh Complex is divided into five tectonic/biostratigraphic units: (1) sedimentary rock unit undivided (Permo-Triassic; Anwar et al. 1993), (2) sedimentary rock unit (Jurassic-Cretaceous; Jones 1961), (3) basalt-chert unit (Early-Late Cretaceous; Kojima et al. 1994), (4) hyaloclastite-mudstone unit (Late Cretaceous; Sawada et al. 1995). and (5) melange unit (Late Cretaceous; Mengal et al. 1994). The volcanic rocks (called here the Hamrani volcanics) are situated at about 12 km south of Muslim Bagh town (Fig. 1) and occur within the hyaloclastite mudstone unit in a narrow strip of Bagh Complex toward north-western margin of Jang Tor Gar Massif of Muslim Bagh Ophiolite (Fig. 1). These volcanic rocks comprise two lenticular bodies of porphyritic and amygdaloidal basalt and hyaloclastite and are found within the Hyaloclastite mudstone unit of the Bagh Complex. The lower basaltic flow is pillowed (30 to 1 m in diameter). The size of the pillow lava body is 30×300 m. The upper body of basaltic flow is massive and 15×150 m in size. The lower contact of the basaltic hyaloclastite is faulted and intercalated with siliceous mudstone and limestone derived from the sedimentary rock unit of Bagh Complex, whereas its upper contact is covered by subrecent to recent alluvial gravel (Fig. 2).

Most of the basalt samples collected from the study area is amygdaloidal. The main textures exhibited by these basalts include porphyritic, cumulophyric, and intersertal. The main minerals identified in these volcanic rocks include titaniferous augite, hornblende, phlogopite, plagioclase ($An_{37–88}$) and devitrified volcanic glass, nosean, and olivine, with aegirine augite in some samples. Apatite, ilmenite, magnetite, and hematite occur as accessories, and chlorite, calcite, stilbite, antigorite, and clay minerals are found as secondary minerals.

Geochemistry

Analytical methods

Ten samples from Hamrani volcanic rocks were analyzed for major and trace elements (Table 1) in the Geoscience

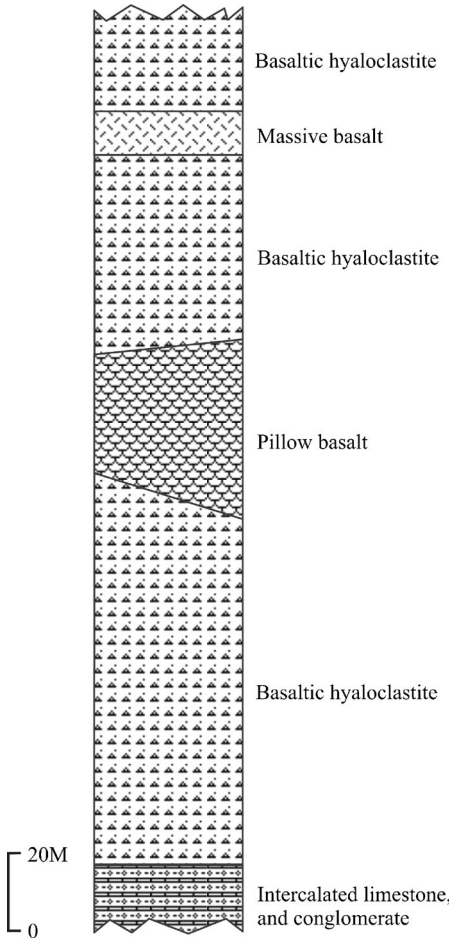

Fig. 2 Generalized stratigraphic sequence of the Hyaloclastite-mudstone unit of Bagh Complex near Hamrani village

Laboratory, Geological Survey of Pakistan, Islamabad, Pakistan. For major elements, the sample powder (<200 mesh) was thoroughly mixed with lithium tetra-borate (flux) with a 1:5 sample flux ratio and the glass beads thus obtained were analyzed on X-ray fluorescence spectrophotometer, RIGAKU 3370E (XRF). For trace elements, powdered pellets of all the samples were prepared by putting 5–7 g powered sample (<200 mesh) in an aluminum cup and compressed between two tungsten carbide plates (within circular briquettes) at about 20 t per square inch pressure, in a hydraulic press. The pellets thus obtained were analyzed on XRF, using corresponding Geological Survey of Japan (GSJ) standard samples with every batch of ten samples. A check of precision of the instrument was made using JA-3 standard sample (Govindaraju 1989).

Geochemical characteristics

The samples from Hamrani are classified on the alkali versus SiO_2 diagram (Fig. 3a) of Le Bas et al. (1986). It can be seen that all the rocks are alkaline and plot in the combined field of basanites and tephrites. In some instances, nonalkaline basalts show high contents of alkalies owing to submarine alteration (e.g., Staudigel 2003). In order to ascertain whether the alkaline character of these rocks is primary or due to alteration, elements considered immobile during alteration were used The Zr/Ti versus Nb/Y diagram, commonly used for the purpose (Fig. 3b), confirms the primary alkaline character of the studied Hamrani volcanic rocks.

It is obvious that the Hamrani volcanic rocks SiO_2 contents were affected by post-magmatic alteration processes. This is also reflected in nonsystematic variations in alkalies and CaO. The Na_2O content in some samples reaches up to 6.43 wt.%, possibly due to albitization. The CaO content is also greatly variable as some of the samples show up to 16.64 wt.% CaO. The presence of calcite in the vesicles suggests that these enrichments can be due to partial replacement of some minerals by calcite. Similarly, the original contents of SiO_2, Al_2O_3, and other major elements may have been changed due to alteration processes and secondary infillings of certain minerals like chlorite, chalcedony, and zeolites in the vesicles. Compared to N-MORB, the Hamrani volcanic rocks show a narrower range of TiO_2 (2.36–3.43) and a wider range of MgO (5.09–7.14). The rocks have low abundances (13.22–16.15 wt.%) of Al_2O_3. They have highly variable concentrations of P_2O_5 (0.68–1.29 wt.%) and have low (48–55) Mg # ($100\times Mg/(Mg+Fe^{2+})$). The major elements of the basalts show enrichment in K_2O, Na_2O, CaO, TiO_2, MnO, and P_2O_5 and depletion in MgO, Fe_2O_3, Al_2O_3, and SiO_2 relative to N-MORB (Tables 1 and 2), which are consistent with the reported values of alkaline rocks (Weaver et al. 1987; Baker 1987).

The Hamrani volcanic rocks are enriched in the whole range of large ion lithophile (LIL) elements (Rb, Sr, and Ba) and high field strength (HFS) elements (Nb, Zr, Ti, and Y) relative to average N-MORB. However, these amounts are consistent with reported values of basaltic alkaline rocks (Tables 1 and 2). The multi-elements spider diagrams are generally used to study the behavior of incompatible trace elements in rocks to constrain their source region with reference to N-MORB, primordial mantle or any other tectonically important composition.

All the samples from the Hamrani volcanic rocks were plotted on primordial mantle-normalized spider diagram (Fig. 3c). Incompatible trace element patterns exhibit variable enrichments of the whole range of trace elements (including LIL elements and HFS elements) relative to both N-MORB and primordial mantle. These patterns also show higher enrichments of LIL elements relative to HFS elements, which are consistent with an enriched mantle source (Pearce 2014). These patterns exhibit marked positive anomalies on Nb, which confirms their origins from an enriched mantle source (e.g., Hofmann 1997).

On OIB-normalized spider plot (Fig. 3d), the Hamrani volcanic rocks exhibit patterns almost parallel to those of OIB, suggesting a source similar to OIB. In the same diagram, all the trace elements are enriched, when compared with N-

Table 1 Whole rocks major oxides and trace elements data of the Hamrani volcanic rocks

Sample	Mb-3	Mb-4	Mb-7	Mb-9	Mb-10	Mb-11	Mb-13	Mb-15	Mb-18	Mb-19
SiO_2	43.40	42.49	39.41	38.63	39.99	39.59	41.06	40.64	41.35	40.84
TiO_2	2.91	2.22	2.96	2.82	3.03	3.00	3.06	3.23	3.19	3.17
Al_2O_3	12.71	12.92	14.37	14.07	14.49	13.96	14.13	14.65	15.18	14.44
Fe_2O_3	12.08	10.19	10.14	9.65	10.26	10.16	10.25	10.87	10.90	10.61
MnO	0.19	0.20	0.17	0.16	0.16	0.15	0.17	0.18	0.17	0.16
MgO	6.86	6.32	5.00	4.81	5.06	4.72	5.03	5.35	5.61	5.20
CaO	11.28	13.30	13.61	14.93	13.88	15.42	14.61	13.70	11.45	13.95
Na_2O	2.06	2.17	4.54	4.45	4.34	3.26	3.17	3.30	4.27	3.35
K_2O	3.39	3.40	1.01	0.79	0.81	1.72	1.74	1.69	1.23	1.69
P_2O_5	0.45	1.24	0.93	0.65	0.63	0.67	0.64	0.68	0.67	0.70
LOI	4.67	5.5	7.8	9.04	7.3	7.1	6.14	5.1	5.98	5
Total	**100**	**99.95**	**99.94**	**100**	**99.95**	**99.75**	**100**	**99.39**	**100**	**99.11**
FeOt	11.17	9.62	9.81	9.43	9.84	9.75	9.71	10.25	10.30	10.02
FeO^t/MgO	1.57	1.43	1.8	1.78	1.8	1.92	1.81	1.81	1.73	1.81
Mg #	53	55	49	50	49	48	49	49	51	49
Ba	1253	1224	295	191	328	366	1009	513	418	323
Rb	53	69	23	20	20	35	36	36	29	35
Sr	662	2200	277	294	318	382	477	443	270	372
Y	45	43	30	28	30	30	29	32	31	31
Zr	455	524	347	334	341	340	337	358	368	358
Nb	114	144	94	92	92	92	89	98	99	98
Ni	135	208	51	47	57	53	59	61	58	62
V	220	187	210	209	213	202	209	216	215	199
Cr	355	302	63	57	74	63	82	92	85	86
Co	49	50	49	48	49	47	49	47	47	47
Ti	18,150	14,136	19,288	18,569	19,587	19,408	19,528	20,546	20,306	20,186
K	29,299	30,046	9130	7221	7221	15,438	15,387	14,857	10,873	14,940
P	5581	4316	3096	3008	3096	3139	2973	3139	3096	3226
Zr/Nb	3.99	3.64	3.69	3.63	3.71	3.70	3.79	3.65	3.72	3.65
Zr/Y	10.11	12.19	11.57	11.93	11.37	11.33	11.62	11.19	11.87	11.55
Y/Nb	0.39	0.30	0.32	0.30	0.33	0.33	0.33	0.33	0.31	0.32
Ti/Zr	39.89	26.98	55.58	55.60	57.44	57.08	57.95	57.39	55.18	56.39
Ti/V	82.50	75.60	91.85	88.85	91.96	96.08	93.44	95.12	94.45	101.44
K/Rb	553	435	397	361	361	441	427	413	375	427
K/Ba	23.38	24.55	30.95	37.81	22.02	42.18	7.42	28.96	26.01	46.25

SiO_2-P_2O_5 are in %, Ba-P are in ppm, Mg #=100×Mg/(Mg+Fe^{+2}), FeOt=total Fe as FeO

MORB. In compatible elements, these rocks are generally greatly variable and low in Cr (57–355 ppm), Ni (47–408 ppm), and Co (47–50 ppm) (Table 1).

Discussion

Nature of parent magma

SiO_2 versus alkali diagram (Fig. 3a) and Zr/Ti versus Nb/Y plot (Fig. 3b) show that the Hamrani volcanic rocks are alkaline. SiO_2 versus Na_2O+K_2O plot (Fig. 4a) further suggest that most of the rocks are mildly to strongly alkaline in nature. The primordial mantle, OIB-normalized spider diagrams (Fig. 3c, d) strongly suggest the derivation of the parent magma from the partial melting of an enriched mantle source. The primordial mantle normalized pattern also shows depletion in Y as compared to other HFS elements. Y is generally partitioned in the garnet, and the depletion of this element in the patterns indicate the presence of residual garnet in the parent magma source (Clague and Frey 1982; Wilson 1989). As mentioned earlier, the OIB-normalized pattern of these

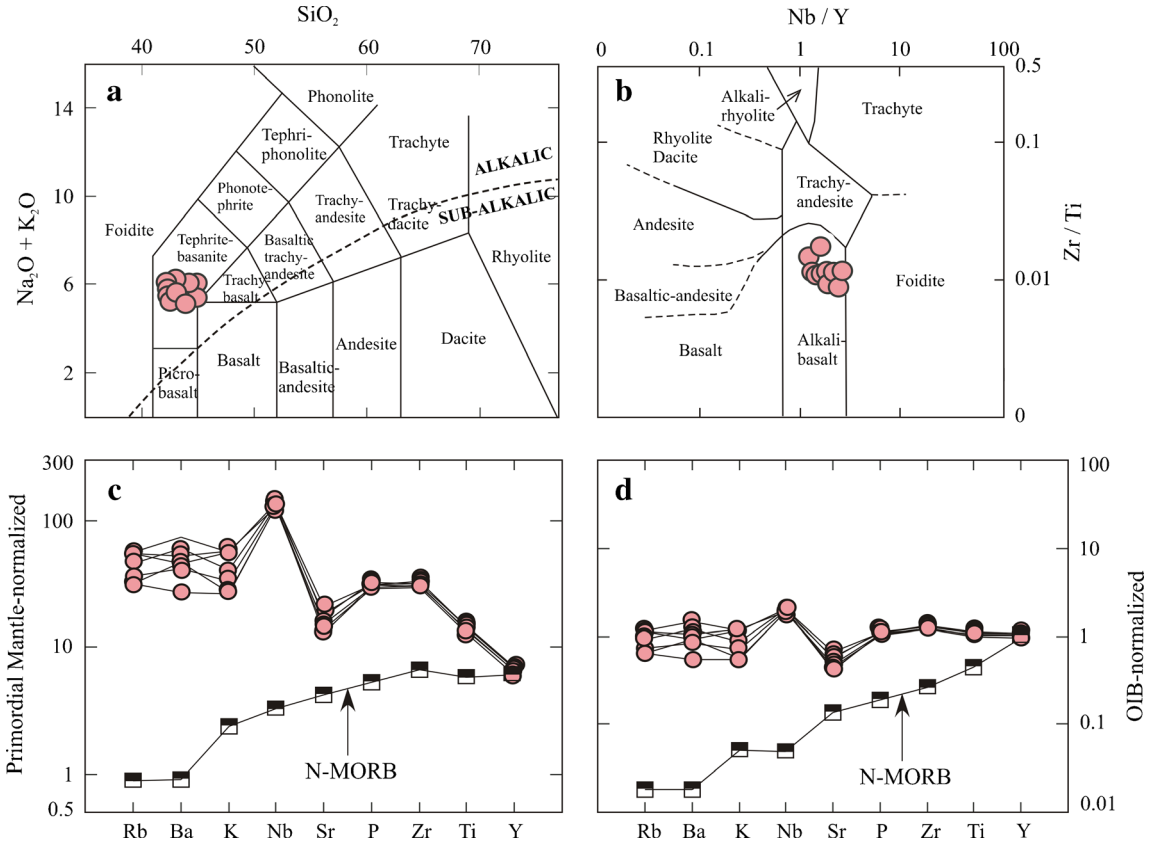

Fig. 3 **a** Alkali versus SiO_2 classification plot (after Le Bas et al. 1986). **b** Zr/Ti versus Nb/Y classification plot (after Pearce 1996). **c** primordial mantle normalized spider diagram; **d** oceanic islands normalized spider diagram. Average N-MORB values in **c** and **d** are after Sun and McDonough (1989)

volcanic are parallel to OIB, indicating a mantle plume-related mantle source.

The Z versus Zr/Y plot (Pearce and Norry 1979) provides useful information about the nature of source, degree of partial melting, and fractionations. Plot in this diagram suggest fractionated nature and about 15 % partial melting of an enriched mantle source for the parent magma. In addition, their Zr/Y (10.11–12.19), Zr/Nb (3.63–3.99), Ti/Zr (26.98–57.95), Y/Nb (0.30–0.39), K/Rb (361–553), K/Ba (07.42–46.25), and Ti/V (75.60–101.44) ratios (Table 1) are consistent with an enriched mantle source (Pearce and Norry 1979; Shervais 1982; Pearce 1983; Wilson 1989; Winter 2001). The aforementioned studies suggest that parent magma of these volcanic rocks was fractionated from a garnet-lherzolite mantle source.

The criteria generally used in support of basaltic rocks being primary melt from a mantle peridotite source or a product of fractionated liquids are (a) presence of mantle peridotite (lherzolite) xenoliths, (b) high magnesium number (Mg #= $100\times Mg/(Mg+Fe2^{+})$) and low FeO_t/MgO ratios, and (c) high contents of compatible elements (Ni, Cr, and Co). The basaltic magma coming from up to 30 % partially melted mantle peridotite source must have Mg # in a range of 68–75 (Green 1976; Frey et al. 1978; Hanson and Langmuir 1978). Gill (1981) has suggested an Mg #≥67, whereas Tatsumi and Eggins (1995) have documented Mg #>70 for primary basaltic magmas. In addition, basalts with Ni (250–300 ppm) and Cr (500–600 ppm) contents are considered to be derived from a primary mantle source (Perfit et al. 1980; Wilkinson and Le Maitre 1987). The Co contents in primary basaltic magma should range from 27 to 80 ppm (Frey et al. 1978)

No mantle lherzolite xenoliths have so far been reported from any of the Muslim Bagh volcanic rocks. The Mg # (48–55), Ni (47–408 ppm), Cr (57–355 ppm), and Co (47–50 ppm) contents in the Hamrani volcanic rocks are well below the values just mentioned for mantle-derived melts (Table 1). It is, therefore, concluded that the Hamrani volcanic rocks are a product of mantle-derived magma that fractionated en route to eruption, mainly due to olivine crystallization.

Tectonic setting

A number of plots and tectonomagmatic discrimination diagrams based on major, minor, or trace elements are designed to study the parent magma and tectonic setting of volcanic rocks. The diagrams based on major elements or LIL elements should be used with caution, as these elements are more mobile during post-magmatic alteration or metamorphic processes as compared to HFS elements (e.g., Weaver et al. 1987; Hastie et al. 2007).

Table 2 Comparison of trace elements and their ratios of Hamrani volcanic rocks with volcanic rocks from Bibai volcanic rocks, N- and E-MORBs, Oceanic islands, Hawaii, Reunion hotspot, and Mount Kenya

Elements and ratios	Hamrani	BIBAI 1	N-MORB 2	E-MORB 3	OIB 4	Reunion 5	Hawaii 6	Mount Kenya 7
SiO_2	43.58	48.06	50.40	51.18	–	47.03	46.40	41.43
TiO_2	3.17	2.54	1.36	1.69	3.35	2.78	2.40	3.64
Al_2O_3	15.09	16.47	15.19	16.01	–	14.38	14.18	11.87
Fe_2O_3	11.24	11.08	10.01	9.40	–	12.81	14.99	15.57
MnO	0.18	0.16	0.18	0.16	–	0.19	0.19	0.23
MgO	5.77	5.98	8.96	6.90	–	8.10	9.47	10.52
CaO	14.58	10.25	11.43	11.49	–	10.96	10.33	11.1
Na_2O	3.75	3.3	2.30	2.74	–	2.60	2.85	2.33
K_2O	1.86	1.75	0.09	0.43	1.12	0.92	0.93	1.48
P_2O_5	0.80	0.42	0.14	0.15	–	0.36	0.28	0.94
Ba	698.50	616	6.3	57	350	210	300	622
Rb	35.60	37	0.56	5.04	31	19	22	52
Sr	570	1003	90	155	660	429	500	1230
Y	32.90	28	28	22	29	29	21	26
Zr	376	189	74	73	280	209	160	197
Nb	101	47	2.33	8.3	48	25	16	59
Zr/Nb	3.72	4.02	31.76	8.80	5.83	8.36	10.00	3.34
Zr/Y	11.47	6.75	2.64	3.32	9.66	7.21	7.62	7.58
Rb/Sr	0.078	0.037	0.006	0.033	0.047	0.044	0.044	0.042
Sr/Y	15.99	35.82	3.21	7.05	22.76	14.79	23.81	47.31
K/Y	449	518.86	21.36	95.09	41.38	263.34	367.62	472.54
Ba/Y	20.75	22.00	0.23	2.59	12.07	7.24	14.29	23.92

Values in column 1 is after Siddiqui et al. 2010; in columns, 2, 3, and 4 after Sun and McDonough 1989; in column 5 after Fisk et al. 1988; in column 6 after Basaltic Volcanism Study Project (1981). and in column 7 is after Price et al. (1985) The major elements in columns 2 and 3 are after Humphris et al. (1985)

The plots of samples from Hamrani volcanic rocks on various discrimination diagrams [Zr/Y versus Nb/Y (Fig. 4b), Nb/Y versus Ti/Y (Fig. 4c), and Ti versus V (Fig. 4d)], involving elements which are considered quite immobile during post-magmatic alteration or metamorphic processes, suggest that these volcanic rocks have an intra-plate origin and are erupted in an OIB setting. This is supported by their spider patterns (Fig. 3c, d) which exhibit enrichment of the whole range of trace elements with marked positive Nb anomalies, confirming their OIB signatures (Saunders and Tarney 1991; Hofmann 1997; Pearce 2014).

Nature of the source of parent magma

The Zr versus Zr/Y plot of Pearce and Norry 1979 (Fig. 5) provides useful information about the nature of source, degree of partial melting, and fractionation. On this diagram, the Hamrani volcanic rocks plot closely to the Reunion hotspot alkali basalts (the ~0–2 Ma; Fisk et al. 1988) suggesting a similar degree of partial melting (about 15 %) from an enriched mantle source for the parent magma, and a similar degree of fractionation for both the volcanic groups.

The marked positive Nb anomalies in the spider diagram (Fig. 3c, d) are explained by the addition of this element in the magma source from the mantle plume (e.g., Hofmann 1997). The positive spikes of certain LIL elements are generally considered to have formed by incorporation of these elements in the source from the upper part of the crust (e.g., Pearce 1982). The spider patterns clearly suggest enriched magma sources for these volcanic rocks.

In Table 2, average trace element chemistry of the Hamrani volcanic rocks are compared with average N-MORB, E-MORB OIB, Reunion hotspot, Bibai volcanic rocks (Siddiqui et al. 2010). Hawaiian and continental rift basalts from the Mount Kenya. The Hamrani volcanic rocks show close similarity with Bibai, Reunion, Hawaii, and Mount Kenya. The source diagnostic ratios (including Zr/Y, Rb/Sr, and Zr/Nb; cf. Floyd 1991) of Hamrani, Bibai, Reunion, Hawaii, and Mount Kenya basalts are similar (Table 2), but K/Y, Sr/Y, and Ba/Y ratios in Hamrani, Reunion, and Hawaii volcanics have lower values, which suggest that the parent magma of the Hamrani volcanic rock was not affected by continental crustal contamination en route to eruption.

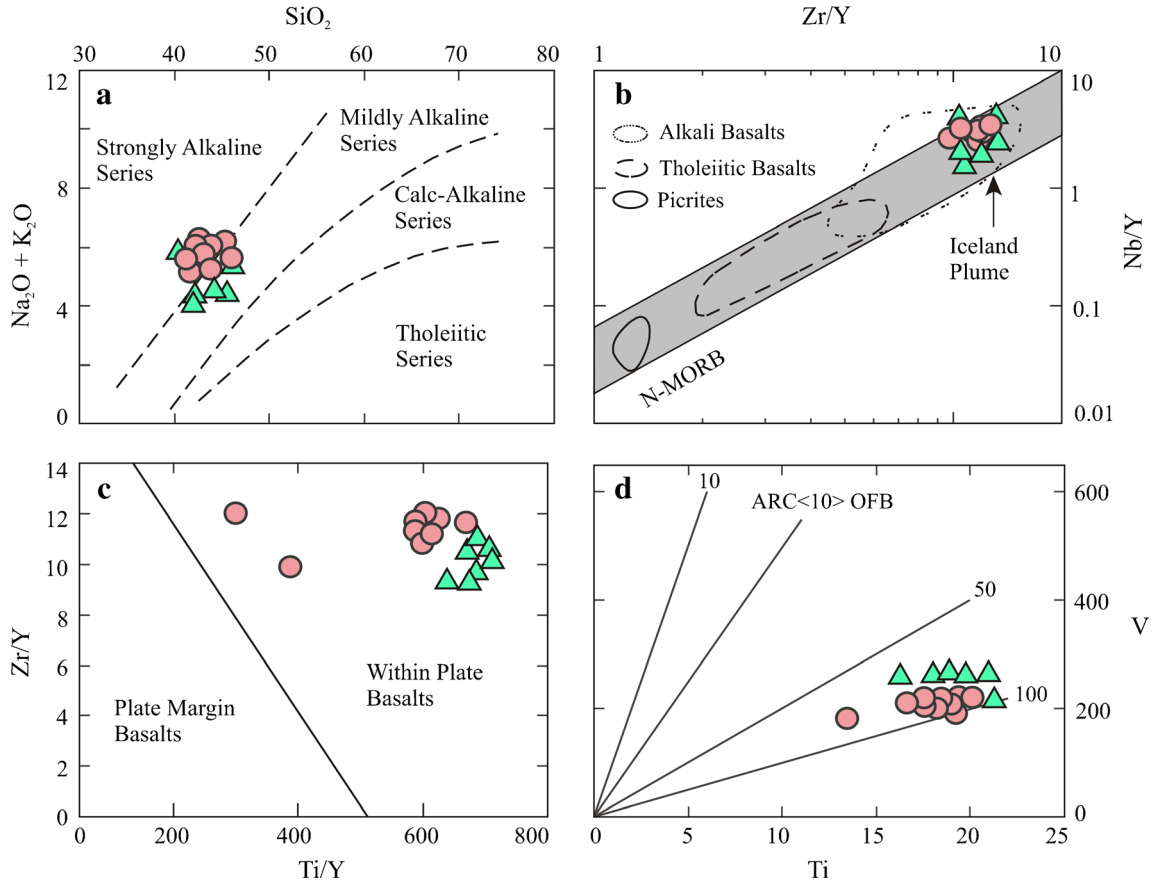

Fig. 4 Tectonic discrimination diagrams of the Hamrani volcanic rocks: **a** Na2O+K2O versus SiO_2 (after Schawarzer and Roger 1974). **b** Zr/Y versus Nb/Y (after Fitton et al. 1997); **c** Zr/Y versus Ti/Y (after Pearce and Gale 1977). **d** Ti versus V (after Shervais 1982). *Filled triangles* are the data from Hamrani volcanic rocks published in Kakar et al. (2014a)

The petrogenetic considerations in the foregoing pages strongly suggests that the Hamrani volcanic rocks represent the intra-plate mantle plume activity possibly of the Reunion hotspot and were erupted during the passage of Ceno-Tethys

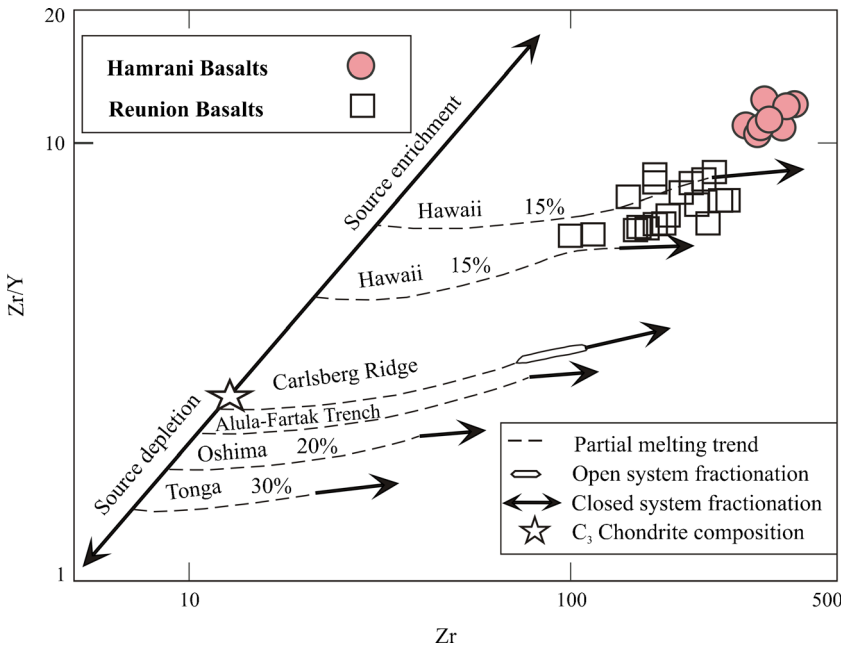

Fig. 5 Zr/Y versus Zr plot of the Hamrani volcanic rocks (after Pearce and Norry 1979). The Reunion hotspot data is from Fisk et al. (1988)

Ocean floor prior to the passage of Indian Plate over it. Sinha and Mishra (1992) have suggested a similar origin for the Late-Cretaceous intra-plate volcanics found in the ophiolite melange in Ladakh, NW Himalaya. Reunion hotspot related

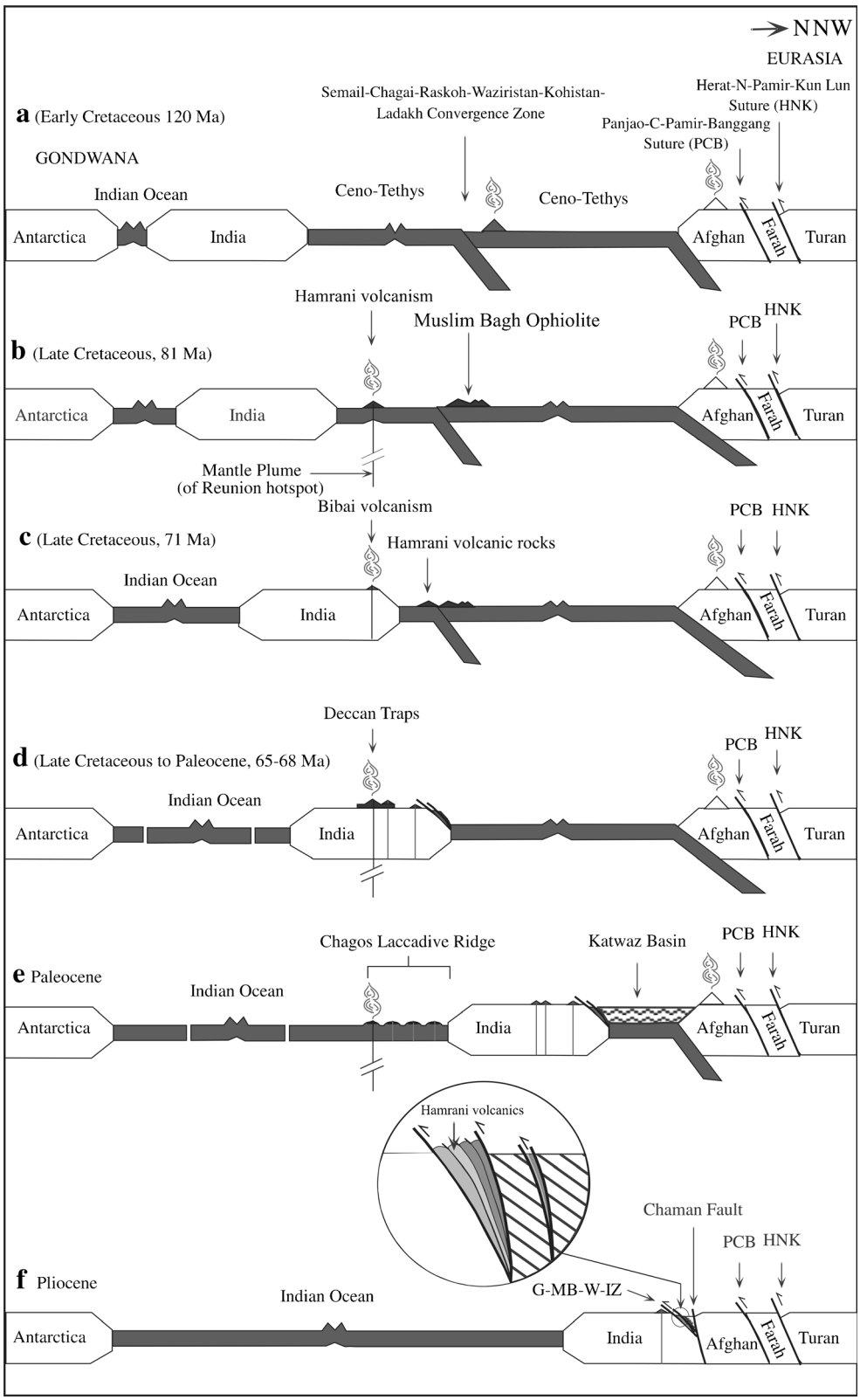

Fig. 6 **a**–**f** Schematic cross sections showing the tectonic evolution of Ceno-Tethys Ocean and the Indian continent from Early Cretaceous to Pliocene (120–05 Ma) (based on the published work of Boulin 1988, 1990; Sengor et al. 1988; Stocklin 1989; Brookfield 1993; Treloar and Izatt 1993; Metcalfe 1995; Zaman et al. 2013; Siddiqui et al. 2010, 2012; Rehman et al. 2011). See the text for further detail

origin for ~71 Ma intra-plates Bibai volcanic rocks in Pakistan is already documented (cf., Khan et al. 1999. Mahoney et al. 2002; Siddiqui et al. 2010; Kerr et al. 2010).

The Reunion Island and the Chagos-Laccadive ridge have been postulated to be formed in a hotspot-related setting (Whitemarsh 1974; Albarede and Tamagnan 1988). Backmann et al. (1989) suggested a hotspot origin for both the Chagos-Laccadive ridge and Deccan basalts. Duncan and Pyle (1988) and Fisk et al. (1988) have documented that the Deccan Trap and the Chagos-Laccadive ridge represent manifestation of Reunion hotspot formed by the passage of Indian continent and Indian Ocean floor during ~68–66 Ma, respectively. The Late Cretaceous to Pliocene (~120–05 Ma) journey of Ceno-Tethys Ocean floor, Indian continent, and Indian Ocean floor is illustrated in Fig. 6a–f. Figure 6a exhibits rifting of India from Gondwana, suturing of Afghan block with Eurasia, intra-oceanic convergence in Ceno-Tethys, and convergence of Ceno-Tethys below the Afghan block. In this figure, two important sutures are also shown including the Late-Triassic Herat-N-Pamir-Kun Lun (between Turan block and Farah block) and Early Cretaceous Panjao-C-Pamir-Banggang (between Farah block and Afghan block). The Turan and Farah blocks were separated from northern margin of Gondwana during Late Devonian and Early Permian and sutured with Eurasia in Early Permian and Late Triassic, respectively (Boulin 1988, 1990; Sengor et al. 1988; Stocklin 1989; Brookfield 1993; Metcalfe 1995; Zaman et al. 2013; Siddiqui et al. 2010, 2012; Rehman et al. 2011). Figure 6b shows eruption of Hamrani volcanic rocks when the Ceno-Tethys Ocean floor passed over the Reunion hotspot in Late Cretaceous (~81 Ma). Figure 6c indicates the eruption ~71 Ma of Bibai volcanic rocks when north-western continental margin of Indian plate passed over this hotspot. Figure 6d represents the Palaeocene (~66 Ma) eruption of Deccan basalt within the Indian continent when it passes over the Reunion hotspot. Figure 6e depicts the obduction of Muslim Bagh Ophiolite and associated Bagh Complex having slivers of Ceno-Tethys Ocean floor accompanying with ~81 Ma Hamrani volcanic rocks on to the north-western margin of the Indian plate during ~55 Ma, formation of Chagos Laccadive in the Indian Ocean floor and initial development of Katawaz basin between Afghan block and Indian plate (e.g., Qayyum et al. 1997; Kasi et al. 2012). Figure 6f shows collision of north-western margin of Indian plate and Afghan block in Pliocene (Treloar and Izatt 1993).

Conclusions

1. This petrogenetic study shows unambiguously that the Hamrani basalts belong to mildly to strongly alkaline intra-plate volcanic rock series.
2. The parent magma of these rock suites was generated by about 15 % partial melting of an enriched mantle source. Their low Mg # and low Cr, Ni, and Co contents suggest that the magma of these volcanic rocks underwent fractionation in an upper level magma chamber, en route to eruption.
3. 3. Geochemical signatures of Hamrani volcanic rocks indicate that their parent magma are not affected by crustal contamination and suggest that these volcanic rocks may have been erupted on the ocean floor of the Ceno-Tethys when it passed over mantle plume. This may represent the earliest stage of impingement of the Reunion hotspot with the lithosphere's base just prior to the migration of Indian Plate across it

Acknowledgments The authors are indebted to S. Hassan Gauhar, Former Director General, Geological Survey of Pakistan, for the arrangement of funds for field and laboratory research. Constructive comments of the reviewer and editors have improved the manuscript substantially. John Foden from the University of Adelaide is thanked for editing the manuscript.

References

Albarede F, Tamagnan V (1988) Modelling the recent geochemical evolution of the Piton de la Fournaise volcano, Réunion Island, 1931–1986. J Petrol 29(5):997–1030

Anwar M, Fatmi AN, Hyderi IH (1993) Stratigraphic analysis of the Permo-Triassic and lower-middle Jurassic rocks from the "axial belt" region of the Northern Baloch1stan, Pakistan. Geol Bull Punjab Univ 28:1–20

Backmann J, Duncan RA et al (1989) Proc ODP Init Rep 115:5–15

Baker BH (1987) Outline of the petrology of the Kenya Rift Alkaline Province. In: Fitten JG, Upton BGJ (eds) Alkaline igneous rocks. Balckwell, Oxford, pp 293–312

Basaltic Volcanism Study Project (1981) Basaltic volcanism on the terrestrial planets. Pergamon Press, New York, p 1286

Boulin J (1988) Hercynian and Eocimmerian events in Afghan and adjoining regions. Tectonophysics 148:253–278

Boulin J (1990) Neocimmerian events in central and western Afghanistan. Tectonophysics 175:285–315

Brookfield ME (1993) The Himalayan passive margin from Precambrian to Cretaceous times. Sediment Geol 84:1–35

Clague DA, Frey FA (1982) Petrology and trace element geochemistry of Honolulu Volcanic Series, Oahu: implication for the oceanic mantle below Hawaii. J Petrol 23:447–504

Duncan RA, Pyle DG (1988) Rapid eruption of Deccan flood basalt at the Cretaceous/Tertiary boundary. Nature 333:841–843

Fisk MR, Upton BGJ, Ford CE (1988) Geochemical and experimental study of the genesis of magmas of Reunion Island, Indian Ocean. J Geophys Res 93:4933–4950

Floyd PA (1991) In: Floyd PA (ed) Oceanic islands and seamounts. Blackie, London

Frey FA, Green DH, Roy SD (1978) Integrated model for basalt petrogenesis: a study of quartz tholeiites to olivine melilite from southeastern Australia, utilizing geochemical and experimental petrological data. J Petrol 19:463–513

Gill JB (1981) Orogenic andesites and plate tectonics. Springer, Berlin

Gnos E, Khan M, Mahmood K, Khan AS, Shafique NA, Villa IM (1998) Bela oceanic lithosphere assemblage and its relation to the Reunion hotspot. Terra Nov. 10:90–95

Govindaraju K (1989) Geostandards newsletter, special issue, working group on analytical standards of minerals, ores and rocks. France 13: 114

Green DH (1976) Experimental studies on a modal upper mantle composition at high pressure under water saturated and water undersaturated conditions. Can Mineral 14:255–268

Hanson GN, Langmuir CH (1978) Modelling of major elements in mantle-melts systems using trace element approaches. Geochim Cosmochim Acta 42:725–742

Hastie AR, Kerr AC, Pearce JA, Mitchell SF (2007) Classification of altered volcanic island arc rocks using immobile trace elements: development of the Co–Th discrimination diagram. J Petrol 48: 2341–2357

Hofmann AW (1997) Mantle geochemistry: the message from oceanic volcanism. Nature 385(6613):219–229

Humphris SE, Thompson G, Schilling JG, Kingsley RA (1985) Petrological and geochemical variation along the Mid Atlantic ridge between 46° S and 32° S: influence of Tristen Da Cunha Mantle Plume. Geochim Cosmochim Acta 49:1445–1464

Jones AG (1961) Reconnaissance geology of part of West Pakistan. A Colombo plan cooperative project. Government of Canada, Toronto

Kakar MI, Kerr AC, Collins AS, Mahmood K, Khan M, McDonald I (2014a) Supra-subduction zone tectonic setting of the Muslim Bagh ophiolite, northwestern Pakistan: insights from geochemistry and petrology. Lithos 202–203:190–206

Kakar MI, Mahmood K, Khan M, Plavsa D (2014b) Petrology and geochemistry of amphibolites and greenschists from the metamorphic sole of the Muslim Bagh ophiolite (Pakistan): implications for protolith and ophiolite emplacement. Arab J Geosci. doi:10.1007/s12517-014-1613-6

Kasi AK, Kassi AM, Umar M, Manan RA, Kakar MI (2012) Revised lithostratigraphy of the Pishin Belt, northwestern Pakistan. J Himal Earth Sci 45(1):53–65

Kerr AC, Khan M, Mahoney JJ, Nicholson KN, Hall CM (2010) Late Cretaceous alkaline sills of the south Tethyan suture zone, Pakistan: initial melts of the Réunion hotspot? Lithos 117:161–171

Khan W, McCormick G R and Reagen M K (1999) Parh Group basalts of northeastern Balochistan, Pakistan: Precursors to the Deccan Traps. In: Macfarlane A Sorkhabi RB, Quade J (eds) Himalaya and Tebbet Mountain roots to Mountain Tops. Geol Soc Ame Spec Publ, pp 59–74

Kimura K, Mengal JM, Siddiqui MRH, Kojima S, Naka T (1993) Geology of the Muslim Bagh ophiolite and associated Bagh complex in northwestern balochistan, Pakistan. Proc Geosci Colloq (abstract) 5:36

Kojima S, Nak T, Kimura K, Mengal JM, Siddiqui RH, Naka T, Bakht MS (1994) Mesozoic Radiolarians from the Bagh Complex in the Muslim Bagh area Pakistan: their significance in reconstructing the geologic history of ophiolites along the Neo Tethys suture zone. Bull Geol Surv Jpn 45(2):63–97

Le Bas MJ, Le Maitre RW, Streckeisen A, Zanettin B (1986) A chemical classification of volcanic rocks based on the total alkali silica diagram. J Petrol 27:745–750

Mahoney JJ, Duncan RA, Khan W, Gnos E, McCormick GR (2002) Cretaceous volcanic rocks of the south Tethyan suture zone, Pakistan: implications for the Réunion hotspot and Deccan Traps. Earth Planet Sci Lett 203:295–310

Mengal JM, Kimura K, Siddiqui MRH, Kojima S, Naka T, Bakht MS, Kamada K (1994) The lithology and structure of a Mesozoic sedimentary-igneous assemblage beneath the Muslim Bagh Ophiolite, Northern Balochistan, Pakistan. Bull Geol Surv Jpn 45: 51–61

Metcalfe I (1995) Gondwana dispersion and Asian accretion. J Geol (Series B): 223–266

Naka T, Kimura K, Mengal JM, Siddiqui RH, Kojima S, Sawada Y (1996) Mesozoic Sedimentary-igneous complex, Bagh Complex in Muslim Bagh area, Pakistan. Proc Geosci Colloq 16:47–94

Otsuki K, Anwar M, Mengal JM, Brohi FA, Hoshino K, Fatmi AN, Okimura Y (1989) Breakup of Gondwanaland and emplacement of ophiolite complex in Muslim Bagh area Balochistan. Hiroshima University Special. Publication, Pakistan, pp 33–57

Pearce JA (1982) Trace elements characterestics of lavas from destructive plate boundaries. In: Throp RS (ed) Andesites: Orogenic andesites and related rocks, John Wiley and Sons, New Yark pp 525–548

Pearce JA (1983) The role of sub continental lithosphere in the magma genesis at destructive plate margin. In: Hawkesworth CJ, Norry MJ (eds) Continental basalts and mantle xenoliths. Shiva:230–249

Pearce JA (1996). A user's guide to basalt discrimination diagrams. In: Wyman DA (ed) Trace element geochemistry of volcanic rocks: applications for massive sulphide exploration. Geological Association of Canada. Short Course Notes 12:79–113

Pearce JA (2014) Immobile element fingerprinting of ophiolites. Elements 10(2):101–108

Pearce JA, Gale GH (1977) Identification of ore- deposition environment from trace element geochemistry of associated igneous host rocks. Geol Soc Spec Publ 7:14–24

Pearce JA, Norry M (1979) Petrogenetic implications of Ti, Zr, Y and Nb variation in volcanic rocks. Contrib Miner Petr 69:33–47

Perfit MR, Gust DA, Bence AE, Arculus RJ, Taylor SR (1980) Chemical characteristics of island arc basalts: implications for mantle sources. Chem Geol 30:227–256

Price RC, Johnson RW, Gray CM, Frey FA (1985) Geochemistry of phonolites and trachytes from the summit region of Mt. Kenya. Contrib Miner Petr 89(4):394–409

Qayyum M, Lawrence RD, Niem AR (1997) Molasse-Delta-flysch continuum of the Himalayan orogeny and closure of the Paleogene Katawaz Remnant Ocean, Pakistan. Int Geol Rev 39(10):861–875

Rehman HU, Seno T, Yamamoto H, Khan T (2011) Timing of collision of the Kohistan–Ladakh Arc with India and Asia: Debate. Island Arc 20:308–328

Saunders AD, Tarney J (1991) Back-arc basins. In: Floyd PA (ed) Oceanic basalts. Blackie, London, pp 219–263

Sawada Y, Siddiqui RH, Aziz A, Rahim SM (1992) Mesozoic igneous activity in Muslim Bagh area, Pakistan, with special reference to hotspot magmatism related to the break-up of the Gondwanaland. Proc Geoscience Coll 12:73–90

Sawada Y, Nageo K, Siddiqui RH, Khan SR (1995) K-Ar ages of the Mesozoic Igneous and metamorphic rocks from the Muslim Bagh area, Pakistan. In Proceedings of Geoscience Colloquium Geoscience Laboratory. Geological Survey of Pakistan 12:73–90

Schawarzer RR, Roger JJW (1974) A Worldwide comparison of alkaline-olivine basalt and their differentiation trends. Earth Planet Sci Lett 23:286–296

Sengor AMC, Altinar D, Cin A, Ustamer T, Hsu KJ (1988) Origin and assembly of Tethyside orogenic collage at the expence of Gondwanaland. In: Charles MGA and Hallan A (eds) Gondwana and Tethys. Geol Soc Spec Pub 37:119–181

Shervais JW (1982) Ti versus V plots and the petrogenesis of modern and ophiolitic lavas. Earth Planet Sci Lett 59:101–108

Siddiqui RH, Brohi IA, Haidar N (2010) Geochemistry petrogenesis and crustal contamination of hotspot related volcanism on the North Western Margin of Indian Plate. SURJ 42(2):15–34

Siddiqui RH, Mengal JM, Hoshino K, Sawada Y, Brohi IA (2011) Back-Arc basin signatures from the sheeted dykes of Muslim Bagh ophiolite complex, balochistan, Pakistan. SURJ 43(1): 51–62

Siddiqui RH, Jan MQ, Khan MA (2012) Petrogenesis of late Cretaceous lava flows from a Ceno-Tethyan island arc: the Raskoh arc, Balochistan, Pakistan. J Asian Earth Sci 59:24–38

Siddiqui RH, Khan MA, Jan MQ, Kakar MI, Kerr AC (2015) Geochemistry and petrogenesis of oligocene volcaniclastic rocks from the chagai Arc: implications for the emplacement of porphyry copper deposits. Arab J Geosci. doi:10.1007/s12517-015-1815-6

Sinha AK, Mishra M (1992) Plume activity and seamounts in Neo-Tethys: evidence supported by geochemical and geochronological data. J Himal Geol 3(1):91–96

Staudigel H (2003) Hydrothermal alteration processes in the oceanic crust. Treatise Geochem 3:511–535

Stocklin J (1989) Tethys evolution in the Afghanistan-Pamir-Pakistan region. In: Sengor (ed) Tectonic evolution of Tethys region. Kluwer Academic Publishers, pp 241–264

Sun SS, McDonough WF (1989) Chemical and isotopic systematics of ocean basalt, implication for mantle composition and processes. In: Saunders AD, Tarney MJ (eds) Magmatism in the ocean basins. Geol Soc Lond Spec Publ 42:313–345

Tatsumi Y, Eggins S (1995) Subduction zone magmatism. Blackwell Science, Oxford

Treloar PJ, Izatt CN (1993) Tectonics of the Himalayan collision between the Indian Plate and the Afghan Block: a synthesis. Geol Soc Lond Spec Publ 74(1):69–87

Weaver BL, Wood DA, Tarney J, Jaron JL (1987) Geochemistry of ocean island basalt from the South Atlantic, Ascension, Bouvet, St. Helena, Gongh and Tristen da Cunha. In: Fitten JG, Upton G (eds) Alkaline Igenous Rocks, pp 253–268

Whitemarsh RB (1974) Summary of general features of Arabian sea and red sea cenozoic history. Based on Leg 23 Cores. Init Rep DSDP 23: 115–1123

Wilkinson JFG, Le Maitre RW (1987) Upper mantle amphiboles and micas and TiO_2, K_2O and P_2O_5 abundances and $100\times Mg / (Mg+Fe^{+2})$ ratios of common basalts and undepleted mantle compositions. J Petrol 28:37–73

Wilson JT (1963) A possible origin of the Hawaiian Islands. Can J Phys 41(6):863–870

Wilson M (1989) Igneous petrogenesis. Unwin and Hyman, London

Winter JD (2001) Igneous and metamorphic petrology. Prentice Hall, New Jersey

Zaman H, Otofuji YI, Khan SR, Ahmad MN (2013) New paleomagnetic results from the northern margin of the Kohistan Island Arc. Arab J Geosci 6(4):1041–1054